Electric Power Systems Research 188 (2020) 106573

Contents lists available at ScienceDirect

Electric Power Systems Research

journal homepage: www.elsevier.com/locate/epsr

Negative sequence quantities-based protection under inverter-based resources − Challenges and impact of the German grid code

Aboutaleb Haddadi[a], Ilhan Kocar[a], Jean Mahseredjian[a], Ulas Karaagac[b], Evangelos Farantatos[c]

[a] Polytechnique Montreal, Montreal, Canada
[b] Department of Electrical Engineering, Hong Kong Polytechnic University, Hong Kong
[c] Electric Power Research Institute, Palo Alto, CA, USA

ARTICLE INFO

Keywords:
Inverter-based resources
Full-scale converter
Wind generation
Short-circuit analysis
Power system protection
Negative-sequence protection
Negative-sequence current injection

ABSTRACT

Inverter-based Resources (IBRs), including Wind Turbine Generators (WTGs), exhibit different negative-sequence fault current characteristics compared to conventional synchronous generators (SGs). Depending on the type and control of IBR, their negative-sequence current contribution can be substantially lower in amplitude and different in phase. Therefore, large-scale integration of IBRs is expected to have a significant impact on negative sequence quantities-based protection elements including Instantaneous Negative Sequence Overcurrent (50Q), Negative Sequence Time Overcurrent (51Q), Directional Negative Sequence Overcurrent (67Q), and fault-identification FID scheme. This paper demonstrates misoperation of these functions in a practical multi wind park system. The misoperation problems are due to the wind parks with full scale converter (FSC) WTGs operating under traditional coupled sequence control (CSC). As illustrated in this paper, such misoperation problems can be eliminated effectively by utilizing a decoupled sequence control (DSC) scheme in FSC WTGs based on the recent VDE-AR-N 4120 Technical Connection Rules.

1. Introduction

Recent technology advancements and continuously decreasing cost of Wind Turbine Generators (WTGs) and solar plants have led to a worldwide increase in the share of renewable energy sources in the generation fleet of power grids [1]. Most commonly, these resources are interfaced to the electrical grid through a power electronic interface and hence in this document are referred to as Inverter-Based Resources (IBRs).

With the increasing share of IBRs, there is an anticipated impact on power system protection [2,3]. The power electronic interface of IBRs produces different, and in some case more complex, fault current signatures compared to conventional synchronous generators (SGs) [4]. Thus, legacy protection elements designed based on the assumption of a SG-dominated power system may not function properly under operating conditions with a high share of power coming from IBRs [5–9]. Such protective relay misoperation problems have been reported, in the context of wind generation, for transmission line ground fault protection [5], power swing protection [6], and distance protection [7–9]. It is important to identify potential protective relay misoperation problems and develop solutions to ensure the proper operation of protection system under high share of IBRs.

The focus of this paper is on protection functions based on negative sequence components. IBRs, especially the ones using full-scale converters (FSC), exhibit different negative-sequence fault current characteristics compared to SGs. Specifically, the amplitude can be substantially lower, and the phase angle can be significantly different. Therefore, protection elements which rely on negative-sequence quantities may not function properly under high levels of IBRs. This paper studies such protection elements as Instantaneous Negative Sequence Overcurrent (50Q), Negative Sequence Time Overcurrent (51Q), and Directional Negative Sequence Overcurrent (67Q), and fault-identification FID scheme. The paper presents case studies illustrating the misoperation of these protection schemes due to FSC based IBRs. Although this paper limits the study to FSC WTGs, the finding and solutions are applicable to all FSC based IBRs.

2. Submitted to the 21st power systems computation conference (PSCC 2020)

To eliminate the misoperation problems, FSC WTG control is modified considering the recent VDE-AR-N 4120 Technical Connection Rules [10] in which the IBRs are required to inject a negative-sequence reactive current during unbalanced faults. This paper evaluates the

E-mail addresses: aboutaleb.haddadi@polymtl.ca (A. Haddadi), ilhan.kocar@polymtl.ca (I. Kocar), jean.mahseredjian@polymtl.ca (J. Mahseredjian), ulas.karaagac@polyu.edu.hk (U. Karaagac), efarantatos@epri.com (E. Farantatos).

https://doi.org/10.1016/j.epsr.2020.106573
Received 1 October 2019; Received in revised form 11 April 2020; Accepted 20 July 2020
Available online 21 July 2020
0378-7796/

effectiveness of this solution in addressing potential protection misoperation issues caused by large-scale integration of FSC WTG. The performance of this solution has been studied under various characteristic gains using simulation tests on a model of a transmission system including wind generation within the EMTP software environment [11].

Reference [12] has presented an implementation of the German grid code. The contributions of this paper with respect to [12] are: i) identifying potential protection misoperation issues in the absence of negative-sequence current injection control; ii) studying the effectiveness of the German grid code in addressing these potential protection misoperation issues; and iii) studying the impact of various factors including proportional gain k and inverter current limits on the negative-sequence behavior of an IBR adopting the German grid code.

3. Fault behavior of inverter-based resources vs. synchronous generator

The negative-sequence fault current response of a SG is characterized by its negative-sequence impedance. Typically, this impedance is small and predominately inductive. As a result, a non-symmetrical power system fault causes a large reactive negative-sequence current to flow through the SG.

Unlike SGs, the negative sequence fault current contribution from IBRs depends highly on their type and control system. The unbalanced fault behavior of doubly-fed induction generator (DFIG) WTs operating under conventional coupled sequence control (CSC) is similar to SGs due to the low impedance path to negative sequence currents provided by the induction generator rotor circuits. On the other hand, the FSC IBR have a very large negative sequence impedance while operating under traditional CSC. Moreover, this apparent impedance can be resistive, inductive or capacitive. It should be noted that negative-sequence fault current response of the DFIG WTs changes significantly when they use decoupled sequence control (DSC) for mitigating torque pulsations. The research presented in this paper is limited to FSC IBR.

To illustrate the difference between FSC IBR and SG unbalanced fault behaviors, a phase-A-to-B fault denoted by AB1 has been simulated in the test system of Fig. 10 (Appendix), and the negative-sequence voltage and current produced by the generator on bus (5), i.e., V2 and I2, have been obtained. Two scenarios have been considered, the first where this generator is a SG, and the second with an FSC WTG plant (WP3 in Fig. 10).

Fig. 1(a) is a plot in the time domain of the amplitude of V2 and I2 under SG, and Fig. 1(b) illustrates the corresponding phasor representation for fault AB1. As shown in Fig. 1(a), prior to the fault the V2 and I2 are zero since in the simulation the grid is considered balanced and operating normally. Following the inception of the fault, the amplitude of V2 increases to approximately 0.33 per-unit (pu). Due to the low negative sequence impedance path provided by the SG, this V2 causes a I2 of about 1.22 pu to circulate through the generator. Fig. 1(b) shows that for the phase-A-to-B fault, I2 leads V2 by 92°. This is due to the predominantly inductive nature of the negative-sequence impedance of the SG.

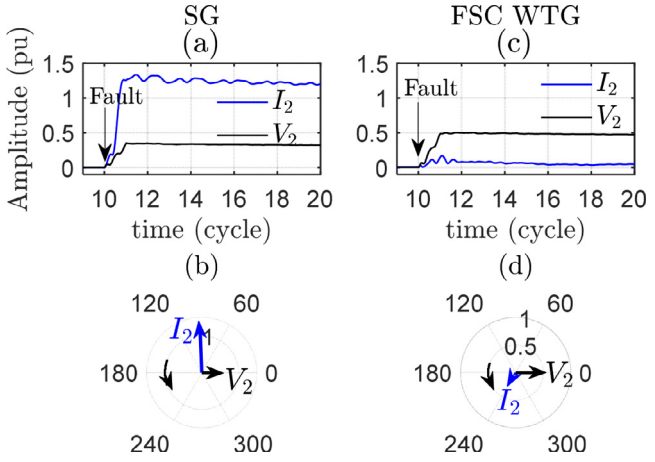

Fig. 1. Negative-sequence voltage and current – SG and FSC scenario.

Fig. 1(c) plots the amplitude of V2 and I2 under FSC WTG, and Fig. 1(d) shows the corresponding phasor representation. As shown, the amplitude of I2 under FSC WTG is about 0.1 pu which is substantially lower than that under SG. Further, the phase angle of I2 with respect to V2 is about 172° under FSC WTG which is different than 92° under SG.

This angular relation as well as the amplitude of negative-sequence quantities are of particular importance for negative sequence-based protection elements. Traditionally, these protection schemes have been designed assuming that the negative sequence quantities are present in significant levels and have an angular relation comparable to the case of SG during unbalanced fault conditions. Given the impact of FSC IBRs on the amplitude and phase angle, protective relays set under the assumption of a conventional SG-dominated power system are likely to mis-operate under operating conditions with a high penetration of IBRs. References [13,14] have shown such a misoperation for 50Q, 51Q, 67Q, and FID scheme. To reduce the likelihood of such protection misoperation problems, a solution is to inject negative-sequence current through the control of IBRs. The next section studies this potential solution.

4. Negative-sequence current injection based on VDE-AR-N 4120

The recent VDE-AR-N 4120 Technical Connection Rules is an example grid code establishing the requirements for negative-sequence current injection of an IBR. Fig. 2 shows the characteristic curve. Under this scheme, the IBR control injects a negative sequence reactive current whose amplitude is proportional to the negative-sequence voltage by a factor "k" defined as the characteristic proportional gain varying between 2 and 6. This characteristic basically emulates the negative-sequence behavior of a SG with 1/k pu negative-sequence reactance (k being the slope of the characteristics) with current rating limitation.

Fig. 3 shows an implementation of the negative-sequence current control based on VDE-AR-N 4120. This scheme is integrated with the current control scheme of the Grid-Side Converter (GSC) and basically calculates current setpoint to achieve a required negative-sequence current characteristic. Reference [15] has presented full details of the rest of control schemes for an FSC WTG. In the figure, the subscripts "1" and "2" denote positive- and negative-sequence component, "*d*" and "*q*" represent the d- and q-axis component, "lv" and "mv" signify the low-voltage and high-voltage side of the Wind Turbine (WT) transformer, and "des" and "ref" represent the desired and reference set points of a signal, respectively.

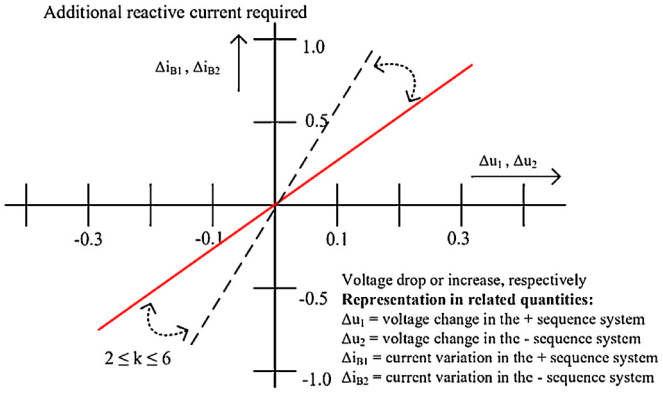

Fig. 2. Characteristic curve for negative-sequence current injection of IBRs based on VDE-AR-N 4120 technical connection rules [10].

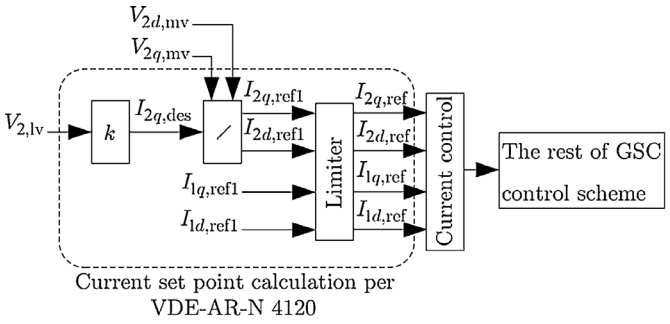

Fig. 3. Integration of VDE-AR-N 4120 with the GSC current control scheme of an FSC IBR.

The objective is to produce a negative-sequence reactive current component I_{2q} whose amplitude is proportional to the amplitude of the negative-sequence voltage $V_{2,lv}$. To that end, first $V_{2,lv}$ is multiplied by the proportional gain k to calculate the desired amplitude of negative-sequence reactive current signified by $I_{2q,des}$. This current is split into a d- and q-axis component denoted by $I_{2d,ref1}$ and $I_{2q,ref1}$ in proportion to the corresponding q- and d-axis component of negative-sequence voltage at the medium voltage side of the WT transformer represented by $V_{2q,mv}$ and $V_{2d,mv}$. Next, the calculated signals $I_{2d,ref1}$ and $I_{2q,ref1}$ together with their positive sequence counterparts $I_{1d,ref1}$ and $I_{1q,ref1}$, supplied by the positive-sequence fault ride-through (FRT) scheme, are sent to a limiter block. This limiter has a logic which operates based on active/reactive current control priority and allocates the total converter current limit to the four input current signals; when operating based on VDE-AR-N 4120, the logic gives the highest priority equally to $I_{2q,ref}$ and $I_{1q,ref}$. This ensures that the control scheme injects a negative-sequence reactive current to comply with VDE-AR-N 4120 and a positive-sequence reactive current to comply with positive-sequence FRT requirements. The next highest priority is given to $I_{2d,ref}$ which produces a negative-sequence real current component. The lowest priority is given to $I_{1d,ref}$ which corresponds to the positive sequence real current.

To illustrate the negative-sequence fault response under VDE-AR-N 4120, fault AB1 of the previous section has been repeated for the FSC WTG scenario assuming k = 6. Fig. 4(a) and (b) show the results. As shown, the amplitude of V2 and I2 become 0.35 pu and 0.71 pu, respectively, and the phase angle of I2 with respect to V2 becomes close to 90° (leading) emulating the behavior of a SG. The results illustrate that the control has successfully increased the amplitude of the negative-sequence fault current contribution of the WTG and produced an inductive phase angle. Note that although the proportional gain is set at k = 6, the effective gain achieved by the controller is smaller due to current limits of the controller.

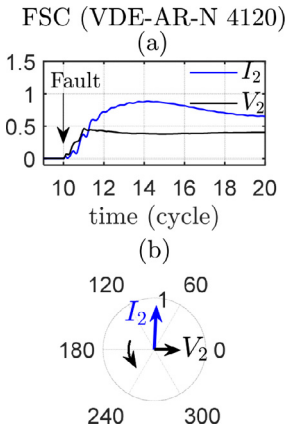

Fig. 4. Negative-sequence voltage and current – FSC incorporating VDE-AR-N 4120 (k = 6).

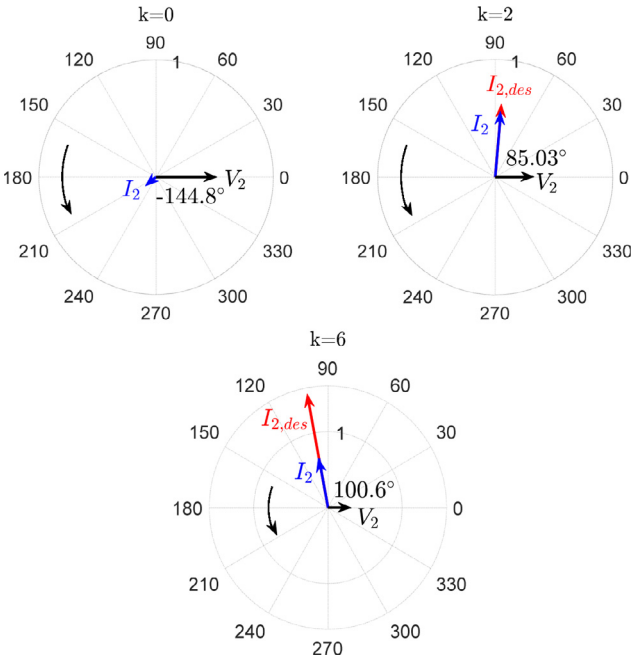

Fig. 5. WTG negative-sequence fault current contribution as a function of proportional gain k: fault AB1.

The amplitude and phase angle of I2 under VDE-AR-N 4120 depend on such factors as the value of k, IBR active/reactive current control priority, and the IBR converter current limit. For proper operation of the protection system, it may be necessary to adjust these parameters to achieve a desired level and phase angle of I2. The next sections study the impact of these factors.

5. Impact of proportional gain k

Gain k determines the amplitude of the injected negative-sequence current, subject to current limits. For smaller values of k, the injected negative-sequence current is linearly proportional to k, and the characteristic basically emulates the negative-sequence behavior of a SG with 1/k pu negative-sequence reactance. For large values of k, the injected negative-sequence current approaches the converter control limit. In this case, the converter may not be able to supply the desired level of negative-sequence current, and the amplitude of the injected negative-sequence current is no longer linearly related to k.

Fig. 5 repeats the simulation of fault AB1 under different values of k and illustrates the negative-sequence fault current and voltage of WP3 in response to fault AB1 as a function of proportional gain k, and Table 1 presents the corresponding GSC current set points. Note that k = 0 corresponds to FSC with no negative-sequence current injection. The total converter current limit has been set at $I_{lim} = 1.1$ pu, and the total active and reactive current limits have been set at $I_{qlim} = 1$ pu and $I_{dlim} = 1$ pu, respectively.

Table 1
GSC current set points for different values of proportional gain k: fault AB1 scenario.

	k = 0	k = 2	k = 6
$V_{2,lv}$ (pu)	0.45	0.29	0.24
$I_{2q,des}$ (pu)	0	0.58	1.44
$I_{2q,ref}$ (pu)	0.00	-0.30	-0.49
$I_{1q,ref}$ (pu)	0.87	0.70	0.51
$I_{2d,ref}$ (pu)	0.00	-0.44	-0.46
$I_{1d,ref}$ (pu)	-0.67	-0.02	-0.00
angle(I_2-V_2) (°)	-144.8	85.0	100.6

As shown, fault AB1 imposes a non-zero $V_{2,lv}$ at the GSC terminal. When k = 0, the GSC control fully suppresses the negative-sequence current by setting $I_{2q,des}$, and hence $I_{2d,ref}$ and $I_{2q,ref}$, to zero. On the other hand, the positive-sequence FRT supplies $I_{1q,ref1} = 0.87$ pu and $I_{1d,ref1} = -0.67$ pu. The limiter does not change these set points since the corresponding amplitude of the positive-sequence current does not exceed the converter current limit of 1.1 pu.

For k = 2, $V_{2,l} = 0.29$ pu causes $I_{2q,des} = 0.58$ pu which is split into $I_{2q,ref1} = -0.41$ pu and $I_{2d,ref1} = -0.44$ pu. The positive-sequence FRT also provides $I_{1d,ref1} = -1.00$ pu and $I_{1q,ref1} = 0.94$pu. These four values are processed by the limiter. The highest priority is given to I_{2q} and I_{1q}; however, since their total amplitude of 1.35 pu exceeds the reactive current limit of 1 pu, they are trimmed to $I_{2q,ref} = -0.30$ pu and $I_{1q,ref} = 0.70$ pu. The remaining current capacity of $\sqrt{1.1^2 - 1^2} = 0.46$ pu is allocated to the active current components, first to I_{2d} and then to I_{1d}. Thus, $I_{2d,ref}$ is set at -0.44 pu which leaves I_{1d} with a very small share of -0.02 pu. These set points produce a negative-sequence current with an amplitude of 0.53 pu and a phase angle of 85.0° leading the negative-sequence voltage. While the negative-sequence proportional gain is 2, the effective gain becomes 1.8 due to current limits.

For k = 6, $V_{2,l} = 0.24$ pu causes $I_{2q,des} = 1.44$ pu which is split into $I_{2q,ref1} = -0.97$ pu and $I_{2d,ref1} = -1.08$ pu. The positive-sequence FRT also provides $I_{1d,ref1} = -1.00$ pu and $I_{1q,ref1} = 1.00$pu. The total amplitude of reactive current is 2.44pu, and hence the reactive current components get limited to $I_{2q,ref} = -0.49$ pu and $I_{1q,ref} = 0.51$ pu. The remaining current capacity is allocated to the active current components; $I_{2d,ref}$ is set at -0.46 pu, and I_{1d} is set at almost 0 pu. These set points produce a negative-sequence current with an amplitude of 0.67 pu and a phase angle of 100.6° leading the negative-sequence voltage. Although the negative-sequence proportional gain is 6, the effective gain becomes 2.8 due to current limits.

Gain k can be designed to increase the level of negative-sequence fault current for proper operation of protection functions such as 50Q and 51Q; however, as the above case studies have shown, the negative-sequence fault current contribution of an FSC IBR cannot be arbitrarily increased by increasing k due to inverter current limits.

6. Impact of inverter current limits

The inverter current limits also impact the amplitude and phase angle of the injected negative-sequence current under the German grid code. To illustrate this, two current limit scenarios have been considered in this section where: (a) the total GSC current limit is set at $I_{lim} = 1.1$ pu, and the d- and q-axis currents have individual limits of $I_{dlim} = 1$ pu and $I_{qlim} = 1$ pu; and (b) the total current limit is set at $I_{lim} = 1.1$ pu with no individual limits on I_d or I_q. In both cases, the proportional gain has been set at k = 4, and fault AB1 has been repeated.

Fig. 6 illustrates the positive and negative sequence voltage and current phasors under the two scenarios. As shown, V2 has both d- and q-axis components, and to inject a reactive I2, the controller should produce both I_{2d} and I_{2q}. For the scenario with I_{lim}, I_{dlim}, and I_{qlim} (Fig. 6 (a)), the controller successfully produces I_{2d} and I_{2q}, and I2 leads V2 by 103.9° which is predominantly inductive. However, in the scenario with I_{lim} only (Fig. 6 (b)), the controller only produces I_{2q} due to the priority of Iq and no individual limit on Iq. With no I_{2d}, the phase angle between I2 and V2 becomes 154.1° which is no longer predominantly inductive. This suggests that in the absence of individual limits on Id and Iq, the injected I2 may not be predominantly inductive. It should be mentioned that in both scenarios I1 is predominantly inductive since V1 only has a d-axis component due to the operation of phase-locked loop (PLL).

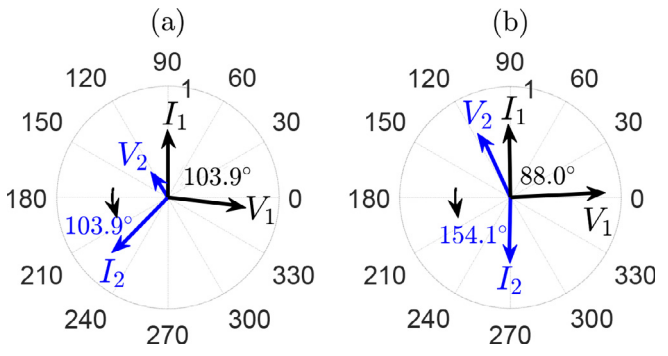

Fig. 6. Unbalanced fault behavior of an IBR adopting the German grid code under two inverter current limit scenarios: (a) $I_{lim} = 1.1$ pu, $I_{qlim} = I_{dlim} = 1$ pu; (b) $I_{lim} = 1.1$ pu with no individual limits on I_d or I_q.

As shown, negative-sequence current control under VDE-AR-N 4120 can increase the level of negative sequence current with desired angular relation of negative-sequence voltages and currents, thereby reducing the likelihood of protection misoperation. The next section studies the performance of various protection elements under this control.

7. Performance of negative sequence quantities-based protection

The case studies of this section evaluate the performance of 50Q, 51Q, 67Q, and FID scheme. Fig. 10 shows the test system and the protective relays used for the tests, and Table 2 presents the parameters and relay settings. The performance of protection system has been studied under three scenarios a) where the generators connected to buses (3), (4), (5), and (9) are SG, b) FSC WTGs, or c) FSC WTG incorporating VDE-AR-N 4120 with proportional gains of k = {6, 6, 6, 2} for WP1, WP2, WP3, and WP4, respectively.

8. Instantaneous negative sequence overcurrent 50Q

A permanent single phase-A-to-ground denoted by AG1 has been placed on the line connecting bus (6) to bus (7). An overcurrent relay R50 on bus (6) containing a 50Q element is used to protect the line. The successful operation requires that 50Q asserts instantaneously.

Fig. 7, Fig. 8, and Fig. 9 show the response of the 50Q element under SG, FSC, and VDE-AR-N 4120 scenarios. As shown, the element asserts successfully under SG since the amplitude of the negative-sequence current is larger than 50Q pick up threshold. However, under FSC WTG the element fails to pick up due to the low level of negative-sequence current. Reference [14] has presented more details about this misoperation and its cause. The misoperation is resolved under VDE-AR-N 4120 due to the increased level of negative-sequence current.

Table 2
Parameters of the test system of Fig. 10.

WP parameters					
WP	Type	Installed capacity	# of units in service	Wind speed	Active power at the POI
WP1	III	200×1.5 MW	100	0.6 pu	32.6 MW
WP2	IV	150×1.5 MW	150	1.0 pu	219.8 MW
WP3	IV	200×1.5 MW	200	1.0 pu	293.0 MW
WP4	IV	133×1.5 MW	133	1.0 pu	194.9 MW
WP5	III	200×1.5 MW	200	0.6 pu	65.2 MW

Settings of relay R50	
Setting	Value
50Q element	
Nominal current	1000 A
Negative-sequence pickup current I_{2pkp}	0.2 pu
67Q element	
Rated current	1000 A
Maximum Torque Angle (MTA)	85°
Forward limit angle	80°
Reverse limit angle	80°
$I_{pkpForward}$	0.25 pu
$I_{pkpReverse}$	0.15 pu

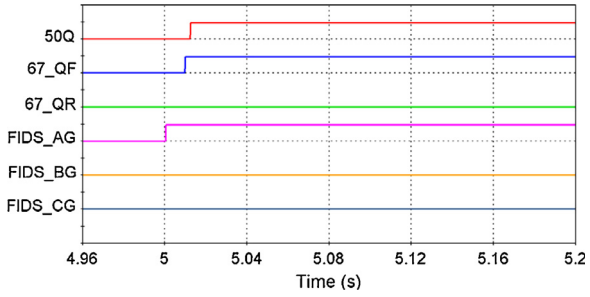

Fig. 7. Relay response to fault AG1– SG scenario.

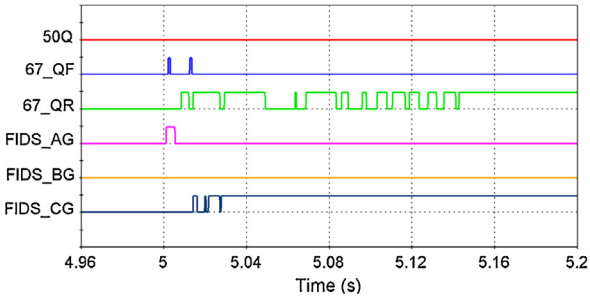

Fig. 8. Relay response to fault AG1– FSC WTG scenario.

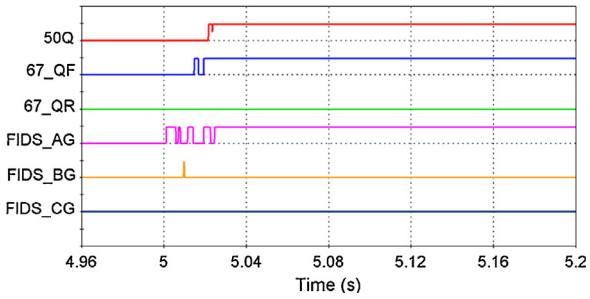

Fig. 9. Relay response to fault AG1– FSC WTG with VDE-AR-N 4120 scenario.

Comparison of Fig. 7 and Fig. 9 reveals that the operation of the 50Q element may have a time delay under the German grid code-controlled IBR compared to that under SG. The reason is the longer rise time of the IBR-injected negative-sequence current due to current controller rise time. Fig. 4 illustrates the rise time of I2; the larger this rise time, the longer would be the delay of 50Q.

9. Directional negative sequence overcurrent 67Q

Fig. 7, Fig. 8, and Fig. 9 also show the response of the 67Q element of relay R50 under SG, FSC, and VDE-AR-N 4120 scenarios. The element uses the phase angle between negative-sequence current and voltage to identify fault direction [16]. The fault is forward to the relay, thus successful 67Q operation requires 67_QF (forward direction) to assert, which is the case under SG. Nevertheless, under FSC 67_QF asserts only transiently, and 67_QR (reverse direction) mistakenly asserts. The cause of this misoperation is the changed phase angle relation of negative-sequence current and voltage which causes the relay to see the fault as reverse. Reference [14] has presented more details about this misoperation. This misoperation is fixed under VDE-AR-N 4120 due to the imposed angular relation between negative-sequence voltage and current of the WTGs.

10. Fault identification

Fig. 7, Fig. 8, and Fig. 9 also show the response of the FID scheme a distance relay denoted by 21R1 on bus (6) looking towards the line. The FID uses the angular relation between the negative- and zero-sequence current to identify the faulted phase [17]. Under SG, the FID successfully detects the faulted phase and issues FIDS_AG. However, due to the changed phase angle of the negative-sequence current under FSC WTG, FID incorrectly classifies the fault as phase-C-to-ground and issues FIDS_CG. Reference [14] has presented more details about this misoperation. This incorrect fault identification is fixed under VDE-AR-N 4120 due to the imposed angular relation between negative-sequence voltage and current of the WTGs.

11. Conclusion

This paper has shown that FSC IBRs may have a detrimental impact on the performance of protection schemes based on negative-sequence quantities. This is due to the lower amplitude of the negative-sequence current contribution of the FSC IBR and the changed angular relation of negative-sequence quantities compared to a conventional SG. The paper has shown the misoperation of 50Q, 67Q, and FID scheme due to FSC WTGs. In the case of 50Q, the cause of misoperation was the low level of negative-sequence current contributed by FSC WTGs. For 67Q and FID, the cause was the changed angular relation. The paper has further shown that FSC WTG negative-sequence current injection can reduce the likelihood of such protection misoperation problems. As an example, the paper has shown the effectiveness of negative-sequence current injection based on VDE-AR-N 4120 in resolving the misoperation of 50Q, 67Q, and FID scheme. The proportional gain of the VDE-AR-N 4120 characteristics (k, with a typical variation range of 2 to 6) is the main factor influencing the negative-sequence fault current behavior of an FSC WTG and hence, can be used as a design parameter to reduce the protection misoperation problems.

Fig. 10 shows the test system consisting of 15 buses marked by (1)-(15) at three voltage levels of {315, 230, 120} kV incorporating 5 Wind Parks (WPs) marked by WP1-WP5. There are two connection points to the rest of the grid represented by Sys1 (at 315 kV level) and Sys4 (at 120 kV level). Minimum loading condition has been considered, and all loads connected to the 25-kV side of the transformers consume 30 MW at unity power factor. Table 2 presents the parameters of the test system.

Declaration of Competing Interest

The authors declare that they have no known competing financial interests or personal relationships that could have appeared to influence the work reported in this paper.

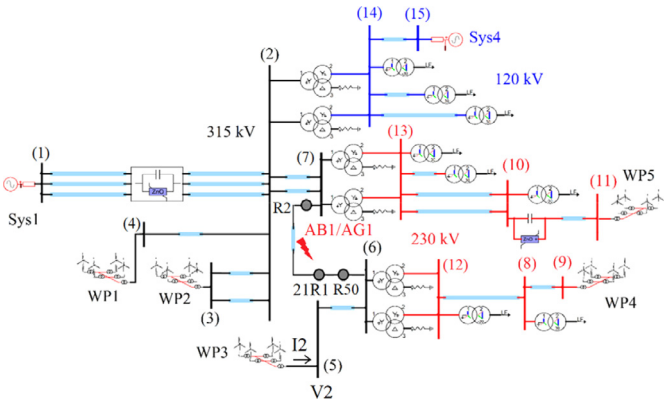

Fig. 10. Test system.

Appendix

Test System

References

[1] U.S. Department of Energy, 2018 Wind Technologies Market Report, Office of Energy Efficiency and Renewable Energy, Aug. 2019 DOE/GO-102019-5191Available online https://www.energy.gov/eere/wind/downloads/2018-wind-technologies-market-report.

[2] IEEE/NERC PES-TR68, "Impact of inverter-based generation on bulk power system dynamics and short-circuit performance", the IEEE/NERC task force on short-circuit and system performance impact of inverter based generation, Jul. 2018.

[3] WSPPID/WSPI/WSPI-P-Wind and Solar Plant Interconnection Performance Working Group (WSPI-P), "P2800-Standard for interconnection and interoperability of inverter-based resources interconnecting with associated transmission electric power systems," PAR approval, Sep. 2018.

[4] IEEE PES Joint Working Group, "Fault current contributions from wind plants," Technical report, Oct. 2013.

[5] M. Nagpal, C. Henville, Impact of power-electronic sources on transmission line ground fault protection, IEEE Trans. Power Deliv. 33 (1) (Feb. 2018) 62–70.

[6] A. Haddadi, I. Kocar, U. Karaagac, H. Gras, E. Farantatos, Impact of wind generation on power swing protection, IEEE Trans. Power Deliv. 34 (3) (Jun. 2019) 1118–1128.

[7] A. Hooshyar, M.A. Azzouz, E.F. El-Saadany, Distance protection of lines connected to induction generator-based windfarms during balance faults, IEEE Trans. Sustain. Energy 5 (4) (Oct. 2014) 1193–1203.

[8] A. Hooshyar, M.A. Azzouz, E.F. El-Saadany, Distance protection of lines emanating from full-scale converter-interfaced renewable energy power plants–Part I: problem statement, IEEE Trans. Power Deliv. 30 (4) (Aug. 2015) 1770–1780.

[9] A. Hooshyar, M.A. Azzouz, E.F. El-Saadany, Distance protection of lines emanating from full-scale converter-interfaced renewable energy power plants – Part II: solution description and evaluation, IEEE Trans. Power Deliv. 30 (4) (Aug. 2015) 1781–1791.

[10] Technische Regeln für den Anschluss von Kundenanlagen an das Hochspannungsnetz und deren Betrieb (TAR Hochspannung), VDE-ARN 4120 Anwendungsregel: 2018-11.

[11] J. Mahseredjian, S. Dennetière, L. Dubé, B. Khodabakhchian, L. Gérin-Lajoie, On a new approach for the simulation of transients in power systems, Elect. Power Syst. Res. 77 (11) (Sep. 2007) 1514–1520.

[12] I. Erlich, T. Neumann, F. Shewarega, P. Schegner, J. Meyer, Wind turbine negative sequence current control and its effect on power system protection, IEEE Power & Energy Society General Meeting, Vancouver, BC, 2013, pp. 1–5.

[13] Protection guidelines for systems with high levels of inverter based resources, EPRI, Palo Alto CA: 2018. 3002013635.

[14] Impact of inverter-based resources on protection schemes based on negative sequence components, EPRI, Palo Alto CA: 2019. 3002016197.

[15] U. Karaagac, et al., A generic EMT-type model for wind parks with permanent magnet synchronous generator full size converter wind turbines, IEEE Power Energy Technol. Syst. J. 6 (3) (Sep. 2019) 131–141.

[16] J. Horak, Directional overcurrent relaying (67) concepts, Proceeding *59 th IEEE Conference for Protective Relay Engineers*, 2006.

[17] D. Costello, K. Zimmerman, Determining the faulted phase, The 63 rd Annual Conference for Protective Relay Engineers, College Station,TX, U.S., Mar. 2010.